INTERNATIONAL TRANSACTIONS ON ELECTRICAL ENERGY SYSTEMS
Int. Trans. Electr. Energ. Syst. (2015)
Published online in Wiley Online Library (wileyonlinelibrary.com). DOI: 10.1002/etep.2089

Nonlinear model reduction-based induction motor aggregation

Gang Zhang*,†, Zhengchun Du, Yu. Ni and Chongtao Li

Department of Electrical Engineering, Xi'an Jiaotong University, Xi'an, 710049, China

SUMMARY

This paper focuses on the problem of aggregating induction motors into a low-order equivalent model, which is very essential in large power system simulations. A new aggregating method is proposed based on nonlinear model reduction technique. The proposed method is developed directly from the detailed dynamic model of induction motors. By using empirical Gramians-based nonlinear model reduction techniques, a low-order load model, which can closely represent the dynamic characteristics of the detailed system, is obtained. The absence of drastic simplifications and the proper preservation of the input–output behavior of the original motors group allow the aggregated model to attain good accuracy. Two case studies are conducted to verify the validity of the proposed aggregating method. The simulation results show that this new method could attain high accuracy of simulation of all the individual induction motors under various operating conditions, especially when system is facing large disturbances. Copyright © 2015 John Wiley & Sons, Ltd.

KEY WORDS: load modeling; motor aggregation; nonlinear model reduction; empirical Gramian; Galerkin projection; adaptive genetic algorithms

1. INTRODUCTION

Numerous investigations have shown that load model is one of the most essential parts in power system stability analysis, and the characteristics of load model have great influence on the transient behavior of the entire power systems [1–3]. Although the importance of load modeling has been well recognized, it is still a challenging task to build the model of loads because of the complexity involved. So far, one of the most widely used load modeling techniques is the component-based method.

The component-based method collects the information on load class mix, on load composition, and on characteristics of load connected to a particular bus. Then after simplification, the load connected to a bus can be seen as a combination of static loads and induction motors. The equivalent load model is acquired by aggregating the induction motor and static load separately.

One of most important and most challenging problems in the component-based approach is the aggregation of induction motors. The load bus may supply a number of induction motors which have different dynamic characteristics and are operating under different conditions. Therefore, it is necessary to develop an effective method to represent a group of induction motors with an equivalent low-order model, which has the same characteristics as the group of the original motors. Over years, a number of methods have been proposed for aggregating induction motors [4,14]. For example, in [4], the parameters of the equivalent motor are calculated as kVA-weighted average of the parameters of each motor (also known as LOADSYN). In [5], the equivalent model is obtained by using a fictitious impedance model based on steady-state models. In [6–8], the parameters of the equivalent motor are determined under two operating conditions, i.e., no-load and locked-rotor conditions. In [9], load rates and critical slips are considered in calculating the kVA-weighted average of the parameters of each motor. In [10], neural network is used in segregating the given group of motors, and parameters of each type of motors are obtained by steady-state model equivalent method. In [11–13], system identification

*Correspondence to: Gang Zhang, Department of Electrical Engineering, Xi'an Jiaotong University, Xi'an 710049, China.
†E-mail: gzhang110@stu.xjtu.edu.cn

techniques are introduced, and the parameters of equivalent motor are obtained directly from the dynamic response seen in simulation. In [14], a new technique for obtaining load model for proper reproducibility of the current during a slow voltage disturbance is presented. In [15], an aggregation algorithm which combining the component-based load modeling method and measurement-based load modeling method is introduced. However, it should be noted that all these aggregation methods listed above focus on calculating parameters of the equivalent load model, and few attention is paid to the structure of load model. In the modeling process of these methods, one equivalent induction motor is used to represent the dynamic behavior of the all the motors connected to a bus. But the load supplied by a substation may consist of induction motors with diverse characteristics. When large disturbances occur in power systems, the accuracy of these methods may deteriorate, and even not acceptable.

In this paper, a procedure for aggregating induction motors is proposed and tested. In this method, the induction motors supplied by a bus are seen from the transmission power system as a nonlinear input–output system. In order to cope with the computation complexity of the high-order dynamic model, empirical Gramian-based nonlinear model reduction technique is used. Empirical Gramians, put forward by Lall [15], are calculated by using simulation trajectories. Furthermore, they can server as an indicator of the importance of each state to the input–output behavior of the system. Based on them, a new system with much lower order can be obtained directly from the detailed model, with good preservation of the dynamic characteristics of the original motors group. Simulation results under different operating conditions are shown to illustrate the efficiency of proposed method.

2. INDUCTION MOTOR AGGREGATION

2.1. Induction motor model

In this paper, the first-order slip model based on the rotor speed is used to describe the dynamics of induction motors. The T-shaped equivalent circuit of induction motor is shown as Figure 1.

where R_1 and R_2 are stator and rotor resistances, respectively; X_1 and X_2 are stator and rotor reactances, respectively, X_m is magnetizing reactance; and s is the slip speed of the rotor.

The model of induction motor is expressed as

$$T_J \dot{s} = T_m - T_e \tag{1}$$

where T_J is the inertia moment, and T_e is the electro-magnetic torque and is given by

$$T_e = \frac{2T_{e\max}}{s/s_{cr} + s_{cr}/s}(U/U_0)^2 \tag{2}$$

and T_m is the applied mechanical torque given by

$$\frac{T_m}{T_{m0}} = a_m\left(\frac{\omega}{\omega_0}\right)^2 + b_m\left(\frac{\omega}{\omega_0}\right) + c_m + d_m\left(\frac{\omega}{\omega_0}\right)^{\gamma} \tag{3}$$

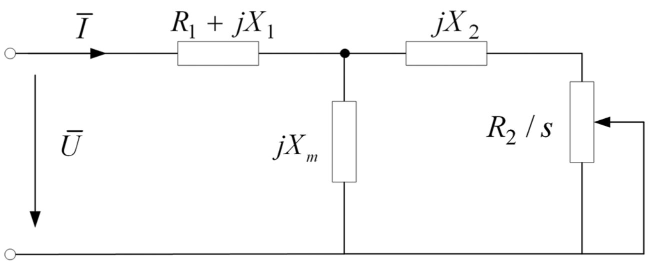

Figure 1. Equivalent circuit of induction motor.

DOI: 10.1002/etep

where a_m, b_m, c_m, and d_m are the mechanical torque characteristic coefficients which satisfy

$$a_m + b_m + c_m + d_m = 1 \tag{4}$$

In the above equations, s_0 is the rated slip, T_{m0} is the initial mechanical torque, $\boldsymbol{U}$ and $\boldsymbol{U}_0$ are the actual and rated terminal voltages of the motor, $T_{e\max}$ is the max electro-magnetic torque under rated terminal voltage, and s_{cr} is the critical slip.

The equivalent impedance of the induction motor is

$$Z = R_1 + jX_1 + jX_m//(R_2/s + jX_2) \tag{5}$$

The power drawn by the motor at any given time can be calculated by

$$\boldsymbol{S} = \boldsymbol{U}^2/Z^* \tag{6}$$

2.2. *Aggregation of induction motors*

In the process of component-based load modeling method, the dynamic load supplied by the bus is seen as a number of induction motors, which is shown in Figure 2. Now consider the aggregation of these motors.

The mathematic model of these motors is given by

$$\begin{cases} \dot{\boldsymbol{s}}(t) = \boldsymbol{f}(\boldsymbol{s}, \boldsymbol{U}) \\ \boldsymbol{y}(t) = Z_1//\cdots//Z_i//\cdots//Z_n \end{cases} \tag{7}$$

where $\boldsymbol{s} = (s_1, s_2, \cdots, s_n)^{\mathrm{T}}$, $\boldsymbol{f}(\boldsymbol{s}, \boldsymbol{u})$ are nonlinear function matrices which are described by Equations (2) and (3), respectively.

The model shown in Equation (7) can be seen as a nonlinear input–output system. The input variable to the system is the bus voltage $\boldsymbol{U}$. The output of the system is the equivalent impedance Z_Σ of the n motors.

The goal of induction motor aggregation is to find a low-order equivalent model, which can preserve the characteristics of detailed dynamic model of induction motors group, as shown in Figure 3.

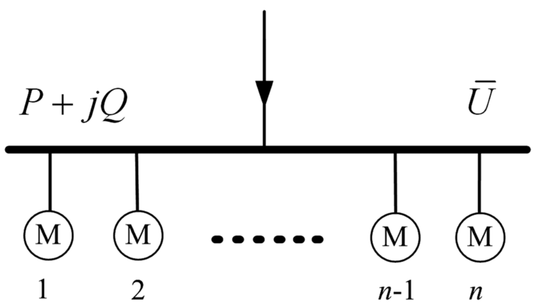

Figure 2. n induction motors system.

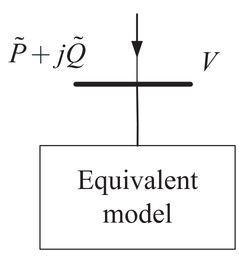

Figure 3. Equivalent load model for n induction motors system.

DOI: 10.1002/etep

3. NONLINEAR MODEL REDUCTION

In this section, an outline of the empirical Gramians-based nonlinear model order reduction technique is given. The model of nonlinear input–output system is

$$\begin{cases} \dot{\boldsymbol{x}}(t) = \boldsymbol{f}(\boldsymbol{x}(t), \boldsymbol{u}(t)) \\ \boldsymbol{y}(t) = \boldsymbol{g}(\boldsymbol{x}(t)) \end{cases} \tag{8}$$

where $\boldsymbol{f}(\mathbf{x}(t), \mathbf{u}(t)) \in \mathbf{R}^n$ and $\boldsymbol{g}(\boldsymbol{x}(t)) \in \mathbf{R}^m$ are nonlinear functions. $\boldsymbol{x}(t) \in \mathbf{R}^n$ is the state of the system, $\boldsymbol{u}(t) \in \mathbf{R}^p$ the input signals, and $\boldsymbol{y}(t) \in \mathbf{R}^m$ the output signals. The objective of the model reduction is to find a lower-order nonlinear input–output system which is expressed by the following equations:

$$\begin{cases} \dot{\tilde{\boldsymbol{x}}}(t) = \tilde{\boldsymbol{f}}(\tilde{\boldsymbol{x}}(t), \boldsymbol{u}(t)) \\ \boldsymbol{y}(t) = \tilde{\boldsymbol{g}}(\tilde{\boldsymbol{x}}(t)) \end{cases} \tag{9}$$

where $\tilde{\boldsymbol{x}}(t) \in \mathbf{R}^r$ and $r < n$. It is expected that the two systems, Equations (8) and (9), have the same input–output behavior. In other words, for the same input $\boldsymbol{u}$, the output $\boldsymbol{y}$ of the system (9) is approximating that of the system (8).

In this section, a method for reducing the order of the nonlinear system of type (8) is presented. Before proceeding further, the balanced truncation for linear system is reviewed briefly, and how it is applied to the nonlinear systems is discussed.

3.1. Balanced truncation for linear system

One of the most effective model reduction methods available today is balanced realization and truncation method proposed by Moore [12]. The idea can be described easily by considering a state space realization of a stable matrix transfer function

$$\boldsymbol{G}(s) = \boldsymbol{C}(s\boldsymbol{I} - \boldsymbol{A})^{-1}\boldsymbol{B} := \left[\begin{array}{c|c} \boldsymbol{A} & \boldsymbol{B} \\ \hline \boldsymbol{C} & \boldsymbol{0} \end{array}\right]$$

where $\mathbf{A}$ is stable. The controllability Gramian $\boldsymbol{W}_c$ and observability Gramian $\mathbf{W}_o$ are the solutions to the following Lyapunov equations:

$$\left\{ \boldsymbol{A}\boldsymbol{W}_c + \boldsymbol{W}_c\boldsymbol{A}^{\mathrm{T}} + \boldsymbol{B}\boldsymbol{B}^{\mathrm{T}} = \boldsymbol{0}\boldsymbol{A}^{\mathrm{T}}\boldsymbol{W}_o + \boldsymbol{W}_o\boldsymbol{A} + \boldsymbol{C}^{\mathrm{T}}\boldsymbol{C} = \boldsymbol{0} \right. \tag{11}$$

The state space realization $(\boldsymbol{A}, \boldsymbol{B}, \boldsymbol{C})$ are said to be balanced if

$$\boldsymbol{W}_c = \boldsymbol{W}_o = \boldsymbol{\Sigma} = \mathrm{diag}\{\sigma_1, , \sigma_2, \cdots, , \sigma_n\}$$

where $\sigma_1 \geq \sigma_2 \geq \cdots \geq \sigma_n \geq 0$. In the case where $(\boldsymbol{A}, \boldsymbol{B})$ is controllable and $(\boldsymbol{C}, \boldsymbol{A})$ is observable, there is always a transformation $\boldsymbol{T}$ such that the transformed state space realization $(\boldsymbol{T}\boldsymbol{A}\boldsymbol{T}^{-1}, \boldsymbol{T}\boldsymbol{B}, \boldsymbol{C}\boldsymbol{T}^{-1})$ is balanced, i.e., $\boldsymbol{T}\boldsymbol{W}_c\boldsymbol{T}^{\mathrm{T}} = \boldsymbol{T}^{-\mathrm{T}}\boldsymbol{W}_o\boldsymbol{T}^{-1} = \boldsymbol{\Sigma}$. Now assume

$$\sum_{i=1}^{r} \sigma_i / \sum_{j=1}^{n} \sigma_j > 95\% \tag{12}$$

and partition the balanced state space realization as

$$\boldsymbol{G}(s) = \left[\begin{array}{cc|c} \boldsymbol{A}_r & \boldsymbol{A}_{12} & \boldsymbol{B}_r \\ \boldsymbol{A}_{21} & \boldsymbol{A}_{22} & \boldsymbol{B}_2 \\ \hline \boldsymbol{C}_r & \boldsymbol{C}_2 & \boldsymbol{0} \end{array}\right], \quad \boldsymbol{A}_r \in \mathrm{R}^{r \times r}$$

Then a reduced order model can be obtained as

$$\boldsymbol{G}_r := \left[\begin{array}{c|c} \boldsymbol{A}_r & \boldsymbol{B}_r \\ \hline \boldsymbol{C}_r & \boldsymbol{0} \end{array}\right]$$

DOI: 10.1002/etep

It was shown that $\boldsymbol{G}_r$ is asymptotically stable, and the approximation error is bounded by

$$||\boldsymbol{G}-\boldsymbol{G}_r||_\infty \leq 2(\sigma_{r+1}+\cdots+\sigma_n)$$

3.2. Empirical Gramians of nonlinear systems

Because it is not suitable to use linear Gramians directly to reduce the order of the nonlinear system, a proper approach has to be devised. Moore proposed a way to calculate the controllability and the observability Gramians based on principal components analysis [16]. The Gramians are obtained by performing principal components analysis on the typical trajectory of the system. Then empirical Gramians of nonlinear system are put forward based on Moore's research [17–22].

For nonlinear system (8), for calculating empirical Gramians, the following sets are defined:

$$\begin{aligned}
&\Upsilon^n=\left\{\Upsilon_1,\ldots,\Upsilon_r\in\mathbf{R}^{n\times n};\Upsilon_i^{\mathrm{T}}\Upsilon_i=\boldsymbol{I},i=1,\ldots,k\right\}\\
&\boldsymbol{M}=\{c_1,\ldots,c_l\in\mathbf{R};c_i>0,i=1,\ldots,l\}\\
&\boldsymbol{E}^n=\{\boldsymbol{e}_1,\ldots,,\boldsymbol{e}_n\}
\end{aligned}$$

where Υ is a set of k orthogonal matrices which define the directions of perturbation. $\boldsymbol{M}$ is a set of l positive constants which define the size of perturbation. $\boldsymbol{e}_i$ is standard unity vector in $\mathbf{R}^n$.

Definition 1: empirical controllability Gramian

Let Υ^p, $\boldsymbol{M}$, and E^p be given sets as described above. p is the number of inputs. The empirical controllability Gramian of system (8) is

$$\hat{\boldsymbol{W}}_c=\sum_{l=1}^{r}\sum_{m=1}^{s}\sum_{i=1}^{p}\frac{1}{rsc_m{}^2}\int_0^\infty\boldsymbol{\Phi}^{ilm}(t)dt \tag{13}$$

where $\boldsymbol{\Phi}^{ilm}\in\mathbf{R}^{n\times n}$ is given by

$$\boldsymbol{\Phi}^{ilm}(t)=\left(\boldsymbol{x}^{ilm}(t)-\overline{\boldsymbol{x}}^{ilm}\right)\left(\boldsymbol{x}^{ilm}(t)-\overline{\boldsymbol{x}}^{ilm}\right)^{\mathrm{T}} \tag{14}$$

and $\boldsymbol{x}^{ilm}(t)$ the state of system (8) corresponding to the unity impulsive input $u(t)=c_m\Upsilon\boldsymbol{e}_i\delta(t)$. $\overline{\boldsymbol{x}}^{ilm}$ is given by

$$\overline{\boldsymbol{x}}^{ilm}=\lim_{T\to\infty}\frac{1}{T}\int_0^T\boldsymbol{x}^{ilm}(t)dt \tag{15}$$

Definition 2: empirical observability Gramians

Let Υ^n, $\boldsymbol{M}$, and E^n be given sets as described above. n is the number of states of the system. The empirical observability Gramian of system (8)

$$\hat{\boldsymbol{W}}_o=\sum_{l=1}^{r}\sum_{m=1}^{s}\frac{1}{rsc_m{}^2}\int_0^\infty\boldsymbol{T}_l\boldsymbol{\Psi}^{lm}(t)\boldsymbol{T}_l{}^{\mathrm{T}}dt \tag{16}$$

where $\boldsymbol{\Psi}^{lm}\in\mathbf{R}^{n\times n}$ is given by

$$\boldsymbol{\Psi}_{ij}^{lm}(t)=\left(\boldsymbol{y}^{ilm}(t)-\overline{\boldsymbol{y}}^{ilm}\right)^{\mathrm{T}}\left(\boldsymbol{y}^{jlm}(t)-\overline{\boldsymbol{y}}^{jlm}\right) \tag{17}$$

where $\boldsymbol{y}^{ilm}(t)$ is the response of system (8) to the initial condition $\boldsymbol{x}_0=c_m\Upsilon\boldsymbol{e}_i$ with input $u(t)\equiv0$. $\overline{\boldsymbol{y}}^{ilm}$ is given by

$$\overline{\boldsymbol{y}}^{ilm}=\lim_{T\to\infty}\frac{1}{T}\int_0^T\boldsymbol{y}^{ilm}(t)dt \tag{18}$$

DOI: 10.1002/etep

The empirical Gramians are obtained from the simulation or experimental data. Because the data is collected within specific regions where the system operates, the empirical Gramians can capture the nonlinear characteristics of the system to some extent.

3.3. *Empirical balanced truncation*

Empirical controllability and observability Gramians are powerful tools for the analysis of input–output behavior of nonlinear systems. The empirical Gramians serve as an indicator for deciding upon the importance of particular subspaces of the state space, with respect to the inputs and outputs characteristics of the system. These Gramians can be used for model reduction of nonlinear systems in the same way as for linear systems as shown before. First, the empirical Gramians are balanced by linear transformation. Then Galerkin projection is performed to obtain the reduced nonlinear system. The algorithm is summarized as follows.

(1) Obtaining the transformation matrix

Let $\hat{\boldsymbol{W}}_c = \boldsymbol{L}_c\boldsymbol{L}_c^{\mathrm{T}}$ and $\hat{\boldsymbol{W}}_o = \boldsymbol{L}_o\boldsymbol{L}_o^{\mathrm{T}}$ be the respective Cholesky factorizations, $\boldsymbol{L}_c^{\mathrm{T}}\boldsymbol{L}_o = \boldsymbol{U\Sigma V}^{\mathrm{T}}$ be the singular value decomposition (SVD) of $\boldsymbol{L}_c^{\mathrm{T}}\boldsymbol{L}_o$. Define the transformation matrix $\boldsymbol{T}$ is

$$\boldsymbol{T} = \boldsymbol{L}_c\boldsymbol{U}\boldsymbol{\Sigma}^{-1/2} \tag{19}$$

The balanced empirical Gramians $\boldsymbol{T}\hat{\boldsymbol{W}}_c\boldsymbol{T}^{\mathrm{T}} = \boldsymbol{T}^{-\mathrm{T}}\hat{\boldsymbol{W}}_o\boldsymbol{T}^{-1} = \boldsymbol{\Sigma}$.

(2) Balanced truncation using Galerkin projection

After it is obtained, the coordinate transformation can be used to find the correspondence between system states and Hankel singular values. The balanced empirical Gramians serve as the indicator of the importance of each state to the dynamic behavior of the nonlinear system. The nonlinear system can then be order-reduced by performing Galerkin projection onto the states corresponding to the largest Hankel singular values.

Galerkin projection is widely used for constructing reduced-order model of nonlinear systems [19]. The main idea is to replace the dynamics of the original system $\boldsymbol{S} \in \mathbf{R}^n$ by the associated ones in a lower-order subspace $\widetilde{\boldsymbol{S}} \in \mathbf{R}^r (r < n)$ of the original state space.

After the transformation of the state space coordinates, the nonlinear system (1) can be truncated by using Galerkin projection.

Define matrix $\boldsymbol{P} = [\boldsymbol{I}, 0] \in \mathbf{R}^{r \times n}$. Applying Galerkin projection leads to the following r-th order nonlinear model

$$\begin{cases} \dot{\tilde{\boldsymbol{x}}}(t) = \boldsymbol{PTf}\left(\boldsymbol{T}^{-1}\boldsymbol{P}^{\mathrm{T}}\tilde{\boldsymbol{x}}(t), \boldsymbol{u}(t)\right) \\ \boldsymbol{y}(t) = \boldsymbol{g}\left(\boldsymbol{T}^{-1}\boldsymbol{P}^{\mathrm{T}}\tilde{\boldsymbol{x}}(t)\right) \end{cases} \tag{20}$$

It can be seen that the method described above actually is to identify the best subspace, without changing the input and output behavior of the system.

4. INDUCTION MOTOR AGGREGATION USING NONLINEAR MODEL REDUCTION

Using the empirical balanced truncation model reduction procedure described in Chapter 3, the reduced order model of the n motors system shown in Figure 2 can be obtained as follows:

(a) Initialization

Choose the sets Υ and M of Equation (3). According to reference [17], the data used to construct empirical Gramians should reflect the dynamic behavior of the system in some given operating region. So, Υ can be defined as $\Upsilon = \{\boldsymbol{I}, -\boldsymbol{I}\}$. The set M gives the number and size of input and states of the system. The elements of M can be chosen according to the magnitudes of the inputs and states seen in simulations to ensure that, during the computation of empirical Gramians, the dynamics would evolve as much as

DOI: 10.1002/etep

possible in the same region where the system is actually operating. The elements of M which are used for finding controllability Gramian are determined based on the range of bus voltage variation in simulations. The elements of M for finding observability Gramian are determined by the critical slip of each motor.

(b) Calculation of Empirical Gramians

Calculate the empirical Gramians $\hat{\boldsymbol{W}}_c$ and $\hat{\boldsymbol{W}}_o$ of n motors system as Equations (13) and (16).

(c) Balancing of the system

Obtain the transformation matrix $\boldsymbol{T}$ using Equation (19), and balance the system.

(d) Truncation

Decide the number r of states to be retained based on the magnitude of the Hankel singular values of the balanced empirical Gramians. According to reference [18], the order r can be chosen by the minimum states that satisfy condition (12).

Then Galerkin projection is applied to obtained the reduced-order system according to Equation (20).

(e) Correction

In order to get more accurate results, nonlinear identification methods are used to modify the reduced system obtained in Step d. In this paper, Adaptive Genetic Algorithm (AGA) [23] is used to modify the transformation matrix $\boldsymbol{T}$ in Equation (20).

In modification, the difference between the output trajectory of the reduced system and that of the original system is chosen as the fitness function of AGA. Then, under typical system inputs, the elements of $\boldsymbol{T}$ will be changed until the minimum value of the fitness function is reached.

5. NUMERICAL TEST RESULTS

To verify the performance and effectiveness of the proposed method, several time domain simulations are carried out in both Anderson system and IEEE 39-bus system. In order to show the capability of the proposed methodology for obtaining accurate load model under various operating conditions, simulations are carried out considering different fault clearing times. In addition, the critical clearing times are also shown to make the comparison more intuitive.

(1) Anderson system

The proposed method was tested on modified Anderson Model containing 3 machines and 9 nodes, as shown in Figure 4. The load model of nodes 6 and 8 is assumed to be constant impedance. For node 5, a combination of dynamic load and constant impedance is used.

The dynamic load supplied by node 5 consists of six different-sized induction motors, of which 42% is residential and 58% is industrial motor load.

The parameters of each motor are given in Table I.

The method proposed in this paper is used to reduce the order of the dynamic load model for the six motors.

First, the empirical Gramians $\hat{\boldsymbol{W}}_c$ and $\hat{\boldsymbol{W}}_o$ of the nonlinear system are calculated. Then the matrix $\boldsymbol{T}$ is obtained through the Gramians. According to Hankel singular values of the balanced Gramians, as shown in Figure 5, the order of reduced system is chosen to be 1 so that the most of the input–output behavior of the detailed system can be retained.

Then the Adaptive Genetic Algorithm is applied. System input of the AGA is shown in Figure 6.

The modified transformation matrix is denoted by $\boldsymbol{T}'$. The reduced system thus obtained becomes

$$\begin{cases} \dot{\tilde{s}}(t) = \sum_{i=1}^{6} \boldsymbol{PT}'(i)\left(T_{mi}(\tilde{s}) - T_{ei}(\tilde{s})\right) \\ \boldsymbol{y}(t) = Z_1//\cdots//Z_i//\cdots//Z_6 \end{cases} \tag{21}$$

DOI: 10.1002/etep

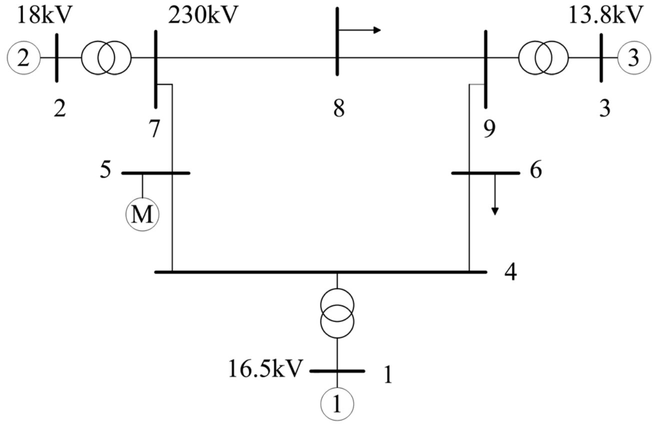

Figure 4. Single line diagram of Anderson system.

Table I. Parameters of induction motors.

R_1	X_1	X_m	R_2	X_2	T_J	A	C	LF	S(MVA)
0.056	0.087	2.4	0.053	0.082	0.56	0.2	0.8	0.5	20.6
0.11	0.14	2.8	0.11	0.065	0.56	1	0	0.5	4.3
0.11	0.12	2	0.11	0.0.13	3	1	0	0.4	8.5
0.12	0.15	1.9	0.13	0.14	2.6	1	0	0.4	8.5
0.031	0.1	3.2	0.018	0.18	1.4	1	0	0.6	31.3
0.013	0.067	3.8	0.009	0.17	3	1	0	0.8	26.8

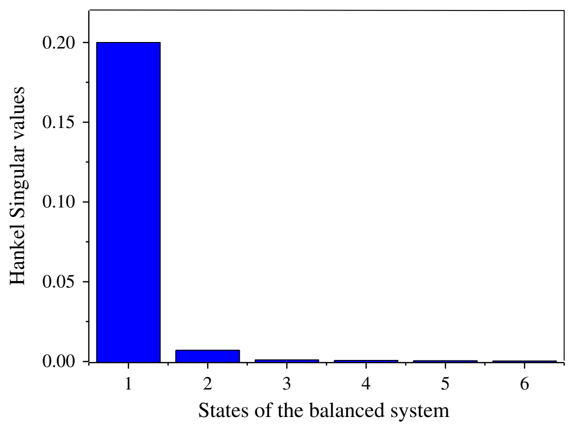

Figure 5. Hankel singular values of the system.

where

$$
\begin{aligned}
T_{mi} &= T_{m0}\left(A\left(1-\boldsymbol{T}^{-1}\boldsymbol{P}(i)\tilde{s}\right)^2/(1-s_0)^2+C\right)\\
T_{ei} &= \frac{2T_{e\max}}{\left(\boldsymbol{T}^{-1}\boldsymbol{P}(i)s\right)/s_{cr}+s_{cr}/\left(\boldsymbol{T}^{-1}\boldsymbol{P}(i)\tilde{s}\right)}(V/V_0)^2\\
Z_i &= R_1+jX_1+jX_m//\left(R_2/\left(\boldsymbol{T}^{-1}\boldsymbol{P}(i)\tilde{s}\right)+jX_2\right)
\end{aligned}
\tag{22}
$$

The reduced system obtained by the method presented in this paper and the equivalent motor obtained by the method of reference [4] and [15] are tested in the Anderson system. Swing curves obtained by these three methods for different fault clearing times are compared to the swing curve of

DOI: 10.1002/etep

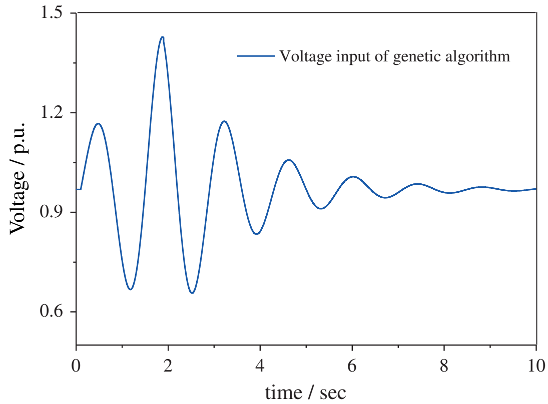

Figure 6. Voltage input of genetic algorithm.

the original six-motor system. The critical clearing time for each method is also given to make the comparison more intuitive.

It is assumed that, at 1 s, a three-phase grounding fault occurred on line 5–7, near bus 7, and is cleared at t_c by the removal of line 5–7.

For $t_c = 110$ms, the generator swing curve and the voltage curve at bus 3 are shown in Figure 7, respectively. It can be seen that the proposed method has better accuracy than the any one of the two methods in reference [4] and [15].

The simulation proceeded with the fault clearing time increasing. For the fault clearing time of 117 ms, the swing curves and bus voltage curve are shown in Figure 8.

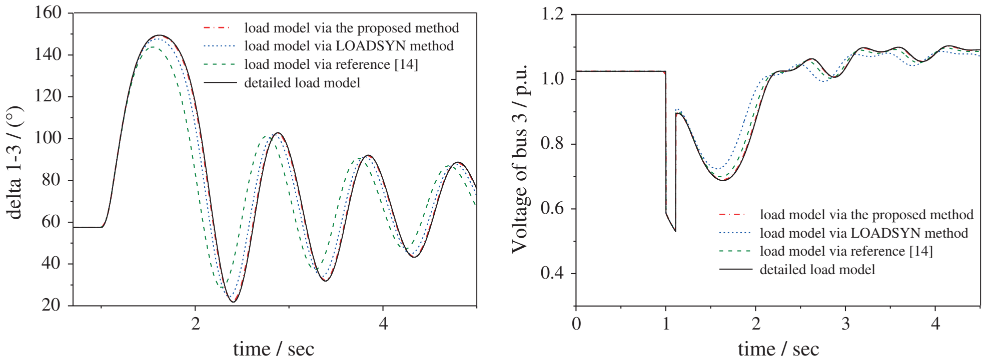

Figure 7. Simulation results for $t_c = 110$ms.

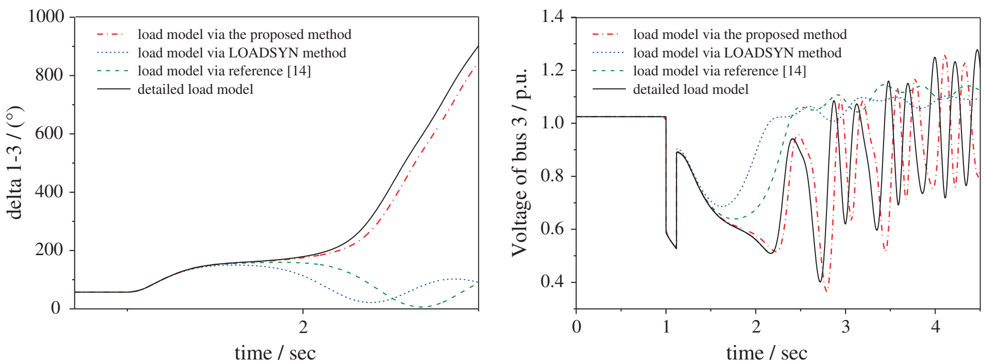

Figure 8. Simulation results for $t_c = 117$ms.

DOI: 10.1002/etep

It is clear in Figure 8 that the original system is unstable if the fault clearance is delayed as late as 117 ms. In this situation, the response of the reduced system is fairly close to that of the original system, but the curves obtained by LOADSYN indicate that the system is stable.

Figure 9 shows the curves for the fault clearing time of 119 ms. In this case, the load model via reference [15] shows unstable results. However, system with load model obtained by LOADSYN is still stable.

Figure 10 shows the curves for the fault clearing time of 124 ms. In this case, all the three load models produced the same conclusion, i.e., the system was unstable.

Table II shows the critical clearing time (CCT) of each load models.

It turns out that the equivalent motor obtained by reference [4] and [15] produces large errors when the system load contains motors with diverse characteristics. Their performance may become even worse when system is operating under critical conditions. The simulation results show that the equivalent motor system remains stable until the fault clearing time increased to 124 ms, even if the CCT for the original system is 116 ms.

The motor aggregation method proposed in this paper is based on nonlinear model reduction and is used to develop a new load model, which, even of much lower order, can achieve high accuracy. It is

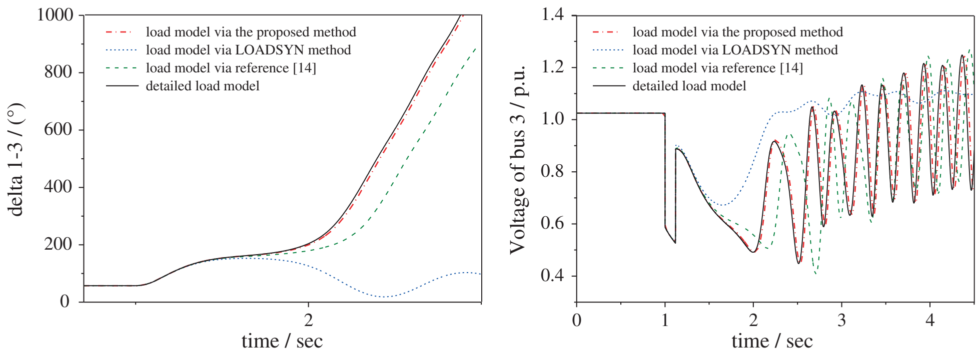

Figure 9. Simulation results for $t_c = 119$ms.

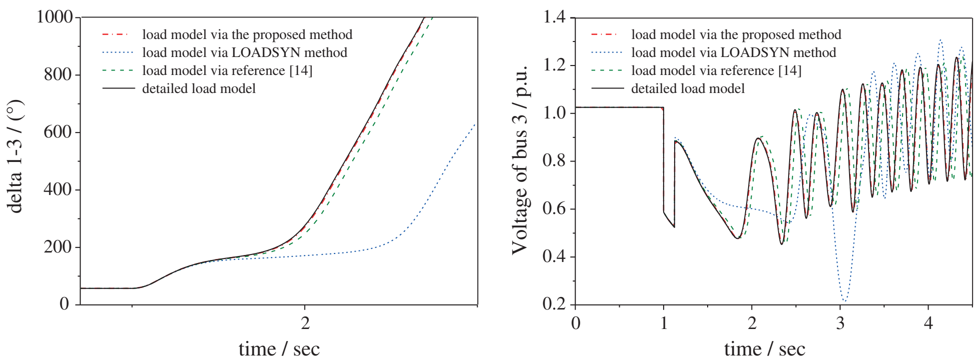

Figure 10. Simulation results for $t_c = 124$ms.

Table II. CCT of each method.

Dynamic load model	CCT (ms)
Original system	116
Load model via nonlinear MOR	116
Load model via LOADSYN	123
Load model via reference [15]	118

DOI: 10.1002/etep

clear from the simulation result that the reduced-order load model could describe the dynamic characteristics as accurately as the original system, especially under some critical conditions.

(2) IEEE 39-bus system.

A similar test is undertaken on a modified IEEE 39-bus system which is shown in Figure 11. This system consists of 46 branches, 10 generators, and 31 load buses. The load models for buses 4 and 15 are assumed to be a group of induction motors paralleled with constant impedance. For other buses, the load is chosen to be constant impedance. The data about the IEEE 39-bus system is given in [1] (Figures 12 and 13).

The parameters of the induction motors connected to bus 4 and 15 are shown in Table III.

The proposed method, together with the methods of reference [4] and [15], is used to obtain the aggregated load model for bus 4 and 15, respectively. According to Hankel singular values shown in Figure 12, the motor group connected to bus 4 can be reduced to an equivalent low-order system of 1st order. For the motors group of bus 15, the Hankel singular values indicate that the order of reduced system needs to be 2 to preserve most of the input–output characteristics of the full order system. By

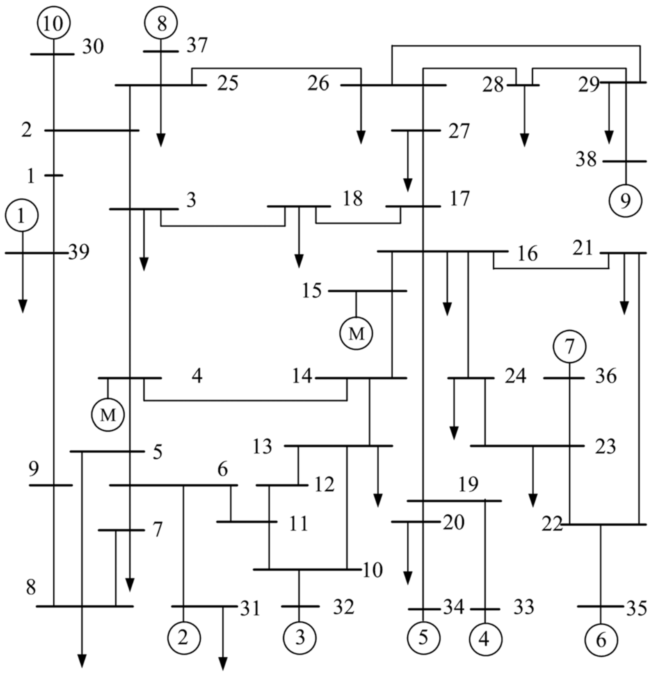

Figure 11. Single line diagram of modified IEEE 39-bus system.

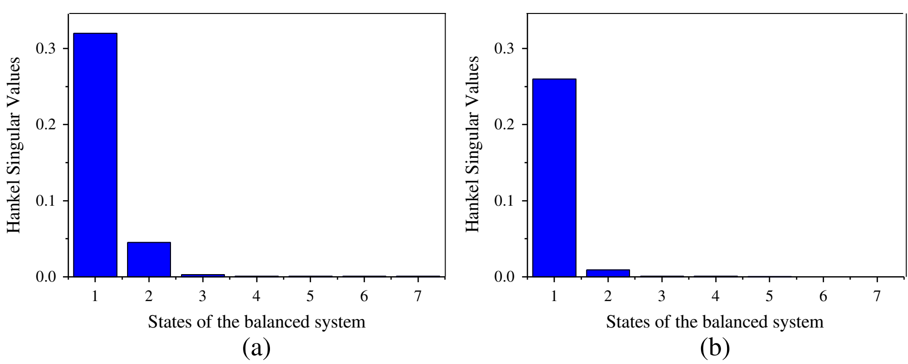

Figure 12. Hankel singular values of the both motors groups: (a) bus 15; (b) bus 4.

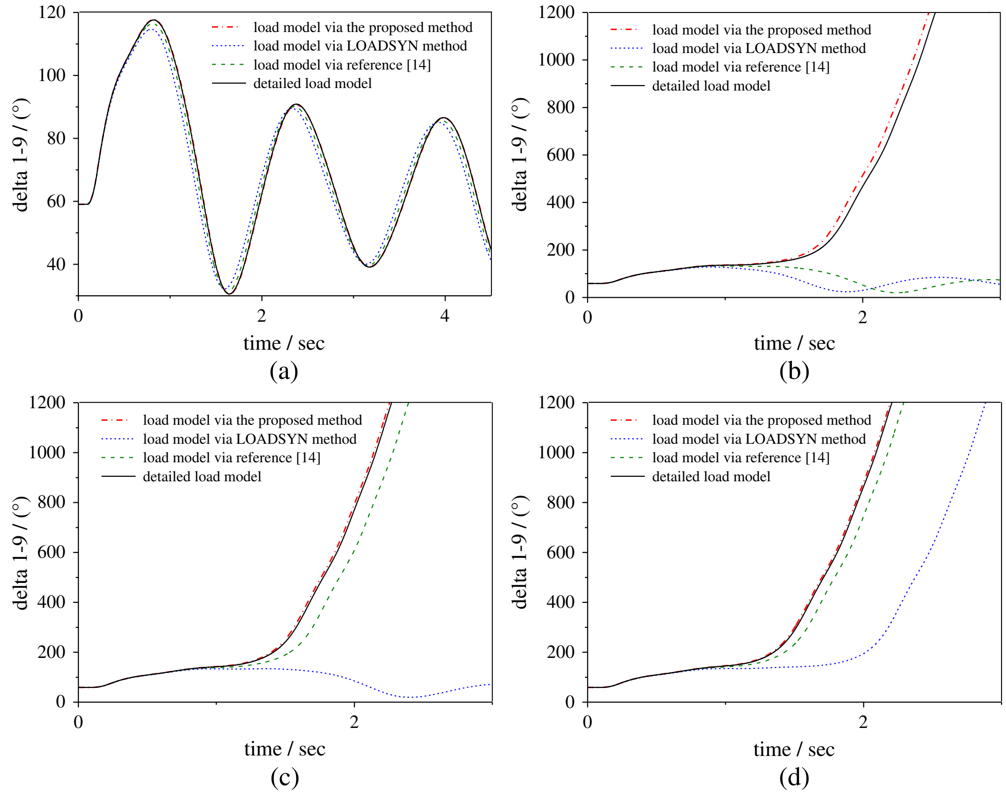

Figure 13. Swing curves for different clearing times: (a) $t_c = 105$ms; (b) $t_c = 116$ms; (c) $t_c = 118$ms; (d) $t_c = 120$ms.

Table III. Parameters of induction motors in New England system.

Bus	R_1	X_1	X_m	R_2	X_2	T_J	A	C	LF	S(MVA)
4	0.016	0.081	2.2	0.029	0.084	1	1	0	0.6	76
4	0.015	0.132	4.0	0.014	0.119	0.6	1	0	0.5	39
4	0.235	0.135	2.58	0.04	0.143	2.8	1	0	0.5	58
4	0.12	0.15	1.9	0.13	0.14	2.6	1	0	0.4	96
4	0.022	0.0795	2.62	0.029	0.104	1.4	1	0	0.6	112
15	0.013	0.067	3.8	0.009	0.17	3	1	0	0.8	50
15	0.033	0.076	2.4	0.048	0.062	0.56	0.2	0.8	0.6	60
15	0.53	0.83	1.9	0.36	0.68	0.56	0.2	0.8	0.6	80
15	0.031	0.14	2.4	0.009	0.12	3	1	0	0.7	50
15	0.077	0.107	2.22	0.079	0.098	1.48	1	0	0.46	40
15	0.035	0.094	2.8	0.048	0.163	1.86	1	0	0.6	100
15	0.064	0.091	2.23	0.059	0.071	0.68	0.2	0.8	0.8	90

using method of reference [2], the motor group of bus 4 is represented by an equivalent motor. For bus 15, because the motors are of diverse characteristics, two equivalent motors are used to achieve better accuracy describing the original motors group.

To validate the derived load model, the contingency is as follows: at 0.1s, a three-phase grounding fault occurred on line 26–28, near bus 28, and is cleared at t_c by the removal of line 26–28.

Swing curves obtained by three methods for different fault clearing times are compared to the swing curve of detailed system. The critical clearing time for each method is also shown in Table IV.

It can be seen from Figure 13 that even of much lower order, the proposed aggregated model can represent the load dynamics of the detailed system in very high accuracy. This simulation of the motor

DOI: 10.1002/etep

Table IV. CCT of each method.

Dynamic load model	CCT (ms)
Original system	115
Load model via nonlinear MOR	115
Load model via LOADSYN	119
Load model via reference [15]	117

aggregation and load modeling based on the complex IEEE 39-bus system shows that the motor aggregation method proposed by this paper has great potential in practice.

6. CONCLUSION

In this paper, a new method for aggregating induction motors is proposed and tested. In this method, the equivalent model is developed directly from the detailed dynamic model of induction motors is directly used. One novelty of this method is that the low-order load model is obtained by applying the empirical Gramian-based nonlinear model reduction techniques to the detailed model of induction motors. A notable feature of the empirical Gramians is that it can capture the input–output behavior of the nonlinear system to some extent. Thus, the new method can achieve high accuracy of describing the dynamic characteristics of a group of different induction motors, even when the system is suffering large disturbance.

Simulations and analysis are carried out on the Anderson system. The results obtained from the proposed aggregation method are compared with those obtained by the method in references for different fault clearing time. The simulations demonstrate that the proposed method yield satisfactory results for various operational conditions.

The main contribution of this paper can be summarized as follows: (i) Different from the single motor equivalent model, the load model in this paper is developed using nonlinear model reduction technique. Based on rigorous mathematical derivation, the proposed aggregated load model can preserve most of the input–output characteristics of the detailed load model. Thus, one of the major advantages of the new method is its high accuracy when aggregating a widely diverse group of induction motors; (ii) The computation procedure is simple and easy to implement. Hence, the proposed method has potential to be applied in the transient simulation of electrical power systems.

7. LIST OF SYMBOLS AND ABBREVIATIONS

7.1. List of symbols

R_1	stator resistance
R_2	rotor resistance
X_1	stator reactance
X_2	rotor reactance
X_m	magnetizing reactance
T_J	inertia moment
T_e	electro-magnetic torque
T_m	applied mechanical torque
a_m, b_m, c_m, d_m	mechanical torque characteristic coefficients
s	slip
s_0	rated slip
T_{m0}	initial mechanical torque
$\boldsymbol{U}$, $\boldsymbol{U}_0$	actual and rated terminal voltages
$T_{e\,\max}$	max electro-magnetic torque under rated terminal voltage
s_{cr}	critical slip.

DOI: 10.1002/etep

Z	equivalent impedance of the induction motor
$\boldsymbol{S}$	power drawn by the motor

7.2. List of abbreviations

AGA	Adaptive Genetic Algorithm
CCT	Critical clearing time

REFERENCES

1. Kundur P. (1994). *Power System Stability and Control* (Vol. **7**). NJ Balu, & MG Lauby (Eds.). New York: McGraw-hill.
2. Abe S, Fukunaga Y, Isono A, *et al*. Power system voltage stability. *Power Apparatus and Systems, IEEE Transactions on* 1982; **10**(11):3830–3840.
3. Price WW, Wirgau KA, Murdoch A, *et al*. Load modeling for power flow and transient stability computer studies[J]. *Power Systems, IEEE Transactions on* 1988; **3**(1):180–187.
4. Nozari F, Kankam MD, Price WW. Aggregation of induction motors for transient stability load modeling. *Power Systems, IEEE Transactions on* 1987; **2**(4):1096–1103.
5. Franklin DC, Morelato A. Improving dynamic aggregation of induction motor models. *Power Systems, IEEE Transactions on* 1994; **9**(4):1934–1941.
6. Karakas A, Li F, Adhikari S. Aggregation of multiple induction motors using MATLAB-based software package. Power Systems Conference and Exposition, 2009. PSCE'09. IEEE/PES. IEEE, 2009: 1–6.
7. Zhang Hongbin, Tang Yong, Zhang Dongxia, Hou Junxian. Study on aggregation of induction motors with distribution network[J]. *Proceedings of the CSEE* 2006; **26**(24):1–4.
8. Zhang H, Liu Q, Liu Y. An aggregation method for induction motor group and its testing with dynamic simulation[J]. *Power System Technology* 2011; **35**(1):96–99.
9. Guo J, Yu Y, Li P, *et al*. An improved weighting-mean aggregation method of induction motors considering load rates and critical slips[J]. *Automation of Electric Power Systems* 2008; **32**(14):6–10.
10. Zhang J, Zhang C, Yan A, *et al*. Aggregation of multi induction motors based on the self-organized neural network and steady state model[J]. *Automation of Electric Power Systems* 2007; **31**(11):44–48.
11. Bai H, Zhang P, Ajjarapu V. A novel parameter identification approach via hybrid learning for aggregate load modeling[J]. *Power Systems, IEEE Transactions on* 2009; **24**(3):1145–1154.
12. Chiang HD, Wang JC, Huang CT, *et al*. Development of a dynamic ZIP-motor load model from on-line field measurements[J]. *International Journal of Electrical Power & Energy Systems* 1997; **19**(7):459–468.
13. Chen Q, Ju P, Shi K Q, *et al*. Parameter estimation and comparison of the load models with considering distribution network directly or indirectly[J]. *International Journal of Electrical Power & Energy Systems* 2010; **32**(9):965–968.
14. Blanes J. Low voltage model for the study of slow disturbances in medium voltage grids[J]. *Electric Power Systems Research* 2013; **99**:64–70.
15. Ju P, Qin C, Wu F, *et al*. Load modeling for wide area power system[J]. *International Journal of Electrical Power & Energy Systems* 2011; **33**(4):909–917.
16. Moore B. Principal component analysis in linear systems: controllability, observability, and model reduction. *Automatic Control, IEEE Transactions on* 1981; **26**(1):17–32.
17. Lall S, Marsden JE, Glavaški S. A subspace approach to balanced truncation for model reduction of nonlinear control systems[J]. *International Journal of Robust and Nonlinear Control* 2002; **12**(6):519–535.
18. Hahn J, Edgar TF. An improved method for nonlinear model reduction using balancing of empirical grammians[J]. *Computers & Chemical Engineering* 2002; **26**(10):1379–1397.
19. Zhang Y, Henson MA, Kevrekidis YG. Nonlinear model reduction for dynamic analysis of cell population models [J]. *Chemical Engineering Science* 2003; **58**(2):429–445.
20. Lall S, Marsden JE, Glavaški S. Empirical model reduction of controlled nonlinear systems[J]. *International Federation of Automatic Control*, 1999; 473–478.
21. Fujimoto K, Scherpen JMA. Singular value analysis and balanced realizations for nonlinear systems. *Model Order Reduction: Theory, Research Aspects and Applications[J]*. Springer: Berlin Heidelberg, 2008; 251–272.
22. Fujimoto K, Scherpen JMA. Balanced realization and model order reduction for nonlinear systems based on singular value analysis[J]. *SIAM Journal on Control and Optimization* 2010; **48**(7):4591–4623.
23. Lu C, Wang R, Chen Y. An adaptive genetic algorithm[J]. *Computer Simulation* 2006; **23**(1):172–175.

DOI: 10.1002/etep